Journal of Environmental Radioactivity 223–224 (2020) 106366

Contents lists available at ScienceDirect

Journal of Environmental Radioactivity

journal homepage: http://www.elsevier.com/locate/jenvrad

^{210}Pb-derived sediment accumulation rates across the Wider Caribbean Region

Ana Carolina Ruiz-Fernández [a], Carlos Alonso-Hernández [b,c], Luisa Fernanda Espinosa [d], Ramón Delanoy [e], Nicolás Solares Cortez [f], Exil Lucienna [g], Ana Carolina Castillo [h], Sheries Simpson [i], Libia Hascibe Pérez-Bernal [a], Yader Caballero [j], Alexis Peña-Castro [k], Fabiola López-Monroy [l], Alberto José Quejido-Cabezas [m], Jesús Antonio Garay-Tinoco [d], Misael Díaz-Asencio [c,n], Miguel Gómez-Batista [c], Juan Pablo Parra Lozano [o], Joan-Albert Sanchez-Cabeza [a,*]

[a] *Universidad Nacional Autónoma de México, Instituto de Ciencias del Mar y Limnología, Mazatlán Academic Unit, Calz. Joel Montes Camarena s/n, Col. Playa Sur, 82040, Mazatlán, Mexico*
[b] *International Atomic Energy Agency, Environment Laboratories, 4 Quai Antoine 1er, 98000, Monaco*
[c] *Centro de Estudios Ambientales de Cienfuegos. Ciudad Nuclear, Cienfuegos, 59350, Cuba*
[d] *Instituto de Investigaciones Marinas y Costeras - INVEMAR, Calle 25 No. 2-55, Playa Salguero, Santa Marta, 470006, Colombia*
[e] *Universidad Autónoma de Santo Domingo, Calle Dr. José Dolores Alfonseca, 10105, Santo Domingo, Dominican Republic*
[f] *Empresa Portuaria Quetzal, Km. 102 Autopista Escuintla-Puerto Quetzal, Escuintla, Guatemala*
[g] *Ministère de l'Environnement, Boulevard des Industries, Port-au-Prince, Haiti*
[h] *Centro de Estudios y Control de Contaminantes, CESCCO/SERNA, Barrio Morazán, Frente a Central de Bomberos, Tegucigalpa, Honduras*
[i] *National Environment & Planning Agency, Jamaica*
[j] *Universidad Nacional Autónoma de Nicaragua, Centro para la Investigación en Recursos Acuáticos, Hospital Monte España 300 Metros al Norte, Managua, Nicaragua*
[k] *Autoridad de los Recursos Acuáticos de Panamá. Edificio La Riviera, Avenida Justo Arosemena y Calle 45 Bella Vista, Ciudad de Panamá, Panama*
[l] *Universidad de Oriente, Núcleo Nueva Esparta, Boca de Río, 6301, Venezuela*
[m] *Centro de Investigaciones Energéticas, Medioambientales y Tecnológicas – CIEMAT, Av. Complutense 40, 28040, Madrid, Spain*
[n] *División de Oceanología, Centro de Investigación Científica y Educación Superior de Ensenada, Carretera Ensenada-Tijuana #3918, Zona Playitas, 22860, Ciudad Ensenada, Baja California, Mexico*
[o] *Ministerio de Minas y Energía, Calle 43 # 57-31, CAN, Bogotá D.C., Colombia*

ARTICLE INFO

Keywords:
^{210}Pb dating
^{137}Cs activities
Sediment accumulation
Historical trends
Gulf of Mexico Large marine ecosystem
Caribbean Sea large marine ecosystem

ABSTRACT

The Wider Caribbean Region is an important tourist destination where agricultural, industrial and shipping activities are also carried on. Coastal zones are heavily populated and receive a high human pressure; however, few monitoring programmes allow assessing long-term anthropogenic impact trends in these areas, which are especially useful for integrated management programs. Through the support of the International Atomic Energy Agency (project RLA/7/012), sediment core activities of ^{210}Pb and ^{137}Cs were used to evaluate changes in sedimentation rates in 11 relevant coastal areas of the region, where environmental information is scarce, but needed to support national environmental policies. Most ^{210}Pb activity profiles were atypical, attributed to non-steady sedimentation conditions; whereas ^{137}Cs activity profiles, showing very low values, were of little help for ^{210}Pb-dating corroboration. Results evidenced conspicuous changes in mass accumulation rates (MAR), specially through the Anthropocene (i.e. since ~1950s) in most cases, attributed to deforestation and land erosion (one of the clearest indicators of global change), and the input of urban and industrial untreated wastes. The recent MAR decrease in Havana Bay (Cuba) was attributed to the implementation of environmental policies, which showed

* Corresponding author.
E-mail addresses: caro@ola.icmyl.unam.mx (A.C. Ruiz-Fernández), C.M.Alonso-Hernandez@iaea.org (C. Alonso-Hernández), luisa.espinosa@invemar.org.co (L.F. Espinosa), radelanoy@gmail.com (R. Delanoy), nicolass1494@puerto-quetzal.com (N. Solares Cortez), exillucienna@yahoo.fr (E. Lucienna), acanavarro24@gmail.com (A.C. Castillo), sheriessimpson@gmail.com (S. Simpson), lbernal@ola.icmyl.unam.mx (L.H. Pérez-Bernal), yadercaballero@cira.unan.edu.ni (Y. Caballero), alexisp@arap.gob.pa (A. Peña-Castro), fametal@gmail.com (F. López-Monroy), alberto.quejido@ciemat.es (A.J. Quejido-Cabezas), jesus.garay@invemar.org.co (J.A. Garay-Tinoco), misaeldiazasencio1971@gmail.com (M. Díaz-Asencio), miguel@ceac.cu (M. Gómez-Batista), jpparra@minenergia.gov.co (J.P. Parra Lozano), jasanchez@cmarl.unam.mx (J.-A. Sanchez-Cabeza).

https://doi.org/10.1016/j.jenvrad.2020.106366
Received 3 April 2020; Received in revised form 29 June 2020; Accepted 20 July 2020
Available online 16 September 2020

that ^{210}Pb-derived reconstruction of environmental changes is also useful to verify the effectiveness of management programs to control land-derived erosion and siltation issues. Since siltation can be detrimental to valuable coastal resources around the world, retrospective evaluations of sedimentation rates, based on ^{210}Pb-dated cores, are highly recommended to assist integrated coastal zone management programs in the region and elsewhere.

1. Introduction

In order to satisfy the needs of natural resources for a rapidly growing human population, the structure and functioning of the Earth system has undergone relevant changes, identified as a whole as *global change*. Among its most conspicuous effects are the loss of vegetation cover and increased continental erosion due to land-use changes (Vitousek, 1994). The perturbations caused by global change are so important that the recognition of the *Anthropocene* as a new geological time unit, starting approximately in the mid 20th century, is under evaluation (AWG, 2019).

Coastal areas, the natural interface between river basins and oceans, are valuable ecosystems but also among the most strongly impacted by global change, because of the large population (more than 2.8 billion people; >40% of the world's population) living within 100 km of the coast (IOC/UNESCO, IMO, FAO, UNDP, 2011). Watershed deforestation is mostly caused by the change in the traditional uses of land (land-use-change, LUC), increasing the sediment flux (causing siltation) and associated particle-reactive contaminants to coastal zones.

The marine environment is the most important natural resource for the countries in the Wider Caribbean Region (WCR), since approximately 60% of the regional Gross National Product depends on its exploitation (e.g. tourism, fisheries, maritime trade). As population and economies expand, the coastal areas are under increasing human pressure owing to land-based sources and activities, importantly LUC due to urbanization and expansion of the agricultural frontier (associated with unsustainable agricultural and forestry practices) and contamination derived from domestic, industrial and agricultural wastes (PNUMA, 2020). However, little information on the long-term effects of coastal siltation in the region is available. Environmental time series are still scarce, short and mostly present in the developed world. To adapt and hopefully mitigate global change, we need to understand its impacts and their temporal evolution during the industrial era, or at least since 1950s, when global change accelerated, especially in the developing world.

The attribution of sedimentary geochemical signals to past events requires a reliable time-frame, that can only be achieved during the Anthropocene through ^{210}Pb dating. Examples of the use of ^{210}Pb dating to study global change in the coastal zone include the reconstruction of temporal trends of erosion and sediment accumulation due to LUC, contamination by metals and organic compounds, and recent climate change (e.g. Ruiz-Fernández et al., 2012; Ruiz-Fernández et al., 2014; Ruiz-Fernández et al., 2016; Cuellar-Martínez et al., 2017).

With the support of the International Atomic Energy Agency (Technical Cooperation project RLA/7/012, "Use of Nuclear Techniques to Address the Management Problems of Coastal Zones in the Caribbean Region"), laboratories of the Marine-Coastal Research Network (Red de Investigación Marino-Costera; REMARCO, 2020) collected and analyzed sediment cores from relevant coastal environments in 11 countries of the WCR, namely Colombia, Cuba, Dominican Republic, Guatemala, Haiti, Honduras, Jamaica, Mexico, Nicaragua, Panama and Venezuela. In this work, we evaluate the temporal trends of ^{210}Pb-derived sediment accumulation rates (SAR) across the WCR, under the hypothesis that the most conspicuous changes in sediment delivery to coastal environments are related to inland human activities throughout the Anthropocene. The conclusions derived from this study might be limited by i) the representativeness of a single core to reconstruct environmental changes at each ecosystem, and ii) problems with the corroboration of the ^{210}Pb chronologies. However, the general patterns observed among the cores and their implications, highlight the need to protect the health of these valuable ecosystems around the WCR region. The information provided is intended to be useful to decision makers to implement national and regional strategies for sustainable coastal zone management.

2. Study area

The IAEA RLA/7/012 project addressed the study of relevant coastal areas, selected by the national counterparts (OIEA, 2020a), where environmental information was scarce but needed to support management plans. The study sites are (Fig. 1):

2.1. Cartagena Bay (Colombia, COL)

Cartagena Bay is located on Colombia's Caribbean coast, between latitudes 10–26°N and 10–16°N, and between longitudes 75-30°W and 75-35°W. It is a semi-closed bay with an average depth of 16 m (Molares and Mestres, 2012). The Dique channel, an artificial arm of the Magdalena river, built in 18th century, discharges freshwater and a large amount of suspended sediments to the bay, transforming it in a heavily stratified estuary (Pagliardini et al., 1982) in which seasonal changes of salinity, dissolved oxygen concentration and other physical, chemical and biological parameters occur (Molares and Mestres, 2012). Cartagena Bay is considered to be one of the Caribbean's hot spots of pollution (Tosic et al., 2019). The input of wastewaters from human settlements (~880,000 inhabitants) and industrial areas of Cartagena (the "Mamonal"), as well as the fluvial discharge of the Magdalena River, which transports eroded soils from its catchment, are considered to be the most important contamination sources to the bay.

2.2. Havana Bay (Cuba, CUB)

Havana Bay (NW Cuba) is a typical enclosed bay, with a mean depth of 10 m, an area of 5.2 km^2 and a water mean residence time of 7–9 days. It receives the fluvial discharges of the Luyano and Martin Perez rivers, and the Tadeo, Matadero, Agua Dulce and San Nicolas streams, as well as untreated effluents from numerous sources. It is adjacent to Havana City (2,130,081 inhabitants in 2016; ONEI, 2017) where industrial, commercial and harbor activities have significantly increased since the middle 19th century, with the onset of industrial activities (e.g. oil refining, electric power and gas production). The area of Havana City experienced a fast economic growth during the 20th century, with a high diversity of industries and commercial activities, and a rapid population growth that required massive urbanization (from 250,000 inhabitants in 1899 to 2.2 million inhabitants in 2001). Agriculture and intensive forest exploitation in the bay catchment (about 68 km^2) has increased soil erosion and, therefore, sediment input to the bay. This ecosystem is considered a hot spot for many contaminants (Díaz-Asencio et al., 2011), causing severe damage to natural resources, owing to the lack of waste treatment facilities (IIT, 1985; Colantonio and Potter, 2006; Valdes-Mujica, 2008; Armenteros et al., 2009). For its location in the Caribbean Region, the area is frequently affected by storms and hurricanes.

2.3. Haina River Estuary (Dominican Republic, DOM)

Haina River (~79 km long, mean annual flow 9.6 m^3 s^{-1}, 564 km^2 catchment area) discharges to the Caribbean Sea through the Haina port, to the west of Santo Domingo (2.9 million inhabitants). Haina port (depth range between ~6 and 11 m; HIT, 2020) was built in 1950s and currently is the primary container port for DOM, the primary entrance point for petroleum products to the country, and an important bulk port of agricultural products (Boske et al., 2001). Around 43% of the Haina River catchment is dedicated to grazing and agriculture (main crops include cocoa, citrus, coffee and coconut) (MMARN, 2020). The waters at the highest part of Haina River basin are considered of good quality, but downstream the river is contaminated by residues from cattle ranching and agriculture, by solid wastes and sewage from human settlements, by industrial wastewaters (e.g. paper mill, sugarcane mill, beer factories, power plants) and by port activities (Gómez-Mena et al., 2008). These contaminated waters make their way to the coastal zone, where coral reefs degradation and loss have been attributed to the turbidity and sedimentation increase promoted by the Haina River (Herrera-Moreno et al., 2009). Located at the Haina River mouth, Haina port suffers continuous silting caused by catchement deforestation (Boske, 2001).

2.4. Amatique Bay (Guatemala; GUA)

Amatique Bay is a shallow semi-enclosed water body (140 km long littoral, ~560 km^2 area and 10 m mean depth; Yañez-Arancibia et al., 1999), connected to the low-lying Lake Izabal and to the Mesoamerican Reef System. It receives fluvial inputs of the rivers Motagua, Sarstún and Dulce, and hosts the ports of Barrios, Santo Tomás de Castilla and Livingston. Red mangrove forests surround the eastern side of Amatique Bay, although large sections of these mangroves were destroyed by Hurricane Mitch in 1998 (Fonseca and Arrivillaga, 2003). The main economic activity is fishing (mainly along the eastern bay) including species of economic importance (e.g. shrimp, squid and demersal fish). It is considered to be the most important estuarine ecosystem in Guatemala and makes part of the Punta de Manabique Ramsar site (# 1016, since 2000). Among the main threats to Amatique Bay and its associated ecosystems are the expansion of grazing, agriculture and tourism activities, as well as contamination resulting from inland erosion, which delivers sediments, agrochemicals and sewage (Yáñez-Arancibia et al., 1999; Andrade et al., 2015; RSIS, 2020b), and hydrocarbon spills owing to shipping activities.

2.5. Port-au-Prince Bay (Haiti, HAI)

Port-au-Prince Bay is a natural harbor adjacent to Port-au-Prince city (2.143 million inhabitants in 2010; ERH, 2019), which hosts ~25% of the total country population. The first port installations were built in 1911 (Noel, 1999) and has a maximum depth of ~20 m. The bay is contaminated by household wastes, sludge from pit latrine and sewage, transported by surface runoff from the city watersheds (Emmanuel and Azaël, 1998). High concentrations of heavy metals have been detected in effluents draining from paint manufacturing facilities and hospitals to the bay (Angerville et al., 2005; Lefranc, 2016). In addition, it receives effluents from the Froide and Gris rivers, the latter carrying waste from distilleries, breweries, automobile workshops and a large agricultural area (bananas, sugar and vegetable crops). The bay is also affected by siltation, promoted by inland soil erosion owing to acute deforestation and vegetation cover loss (UNEP, 1999), which started from the beginning of the 19th century, since the country had to sell huge quantities of wood, especially mahogany, to pay a debt acquired in exchange of its independence. Deforestation continues today, since nearly 80% of the population uses wood as a source of energy (UNEP, 2010).

2.6. Puerto Cortés Bay (Honduras, HON)

Puerto Cortés Bay hosts the Central America's largest port, located at a deep natural harbor (maximum depth ~14 m), adjacent to the coastal city of Puerto Cortés, considered a growth pole in Honduras. The population of the city is ~132,000 inhabitants and it is rapidly growing (INE, 2018). The main sources of pollution are the manufacturing industry, agriculture and commercial activities, including the input of oil residues generated by the port activities; contaminated soils, eroded as a result of LUC for agriculture and cattle raising; and domestic and industrial wastewaters through the rivers Tulián, Medina and

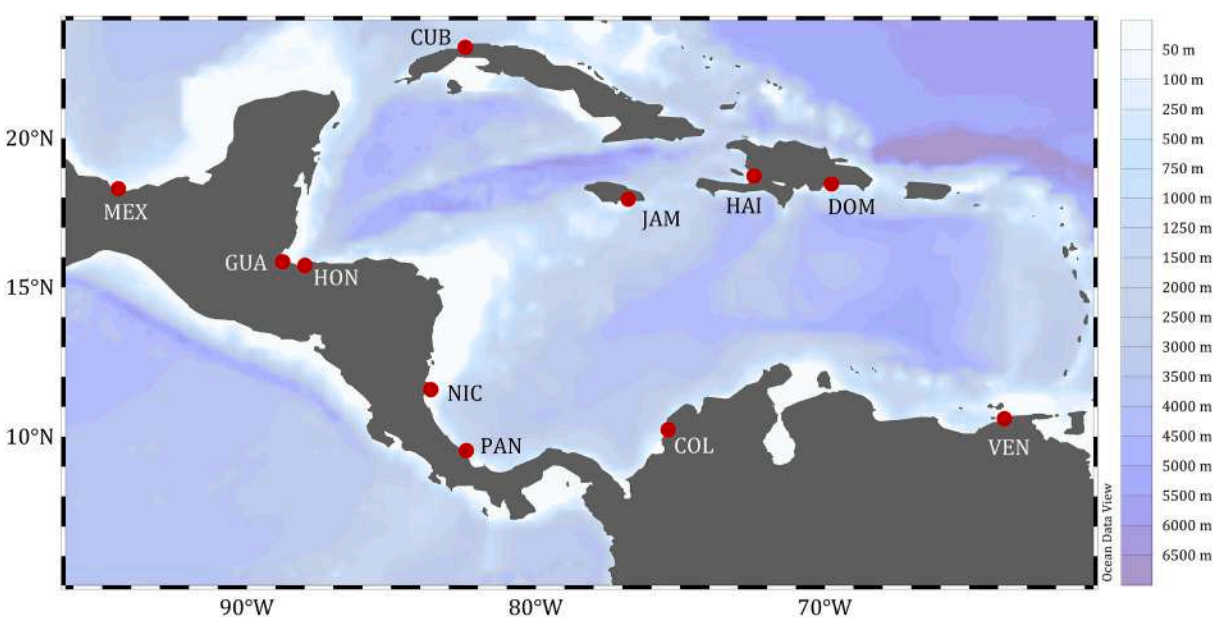

Fig. 1. Sediment core collection sites in the Wider Caribbean Region. The site and sampling coordinates (latitude, longitude; in decimal degrees) where each core was collected are in parenthesis. COL (Cartagena Bay, Colombia; 10.36°N, −75.52°W), CUB (Havana Bay, Cuba; 23.14°N, −82.33°W), DOM (Haina River Estuary, Dominican Republic; 18.41°N, −70.02°W), GUA (Amatique Bay, Guatemala; 15.90°N, −88.71°W), HAI (Port-au-Prince Bay, Haiti; 18.55°N, −72.37°W), HON (Puerto Cortés Bay, Honduras; 15.81°N, −87.97°W), JAM (Kingston Harbour, Jamaica; 17.96°N, −76.74°W), MEX (Coatzacoalcos River Estuary, Mexico; 18.24°N, −94.45°W), NIC (Bluefields Bay, Nicaragua; 11.88°N, −83.75°W), PAN (Almirante Bay, Panama; 9.28°N, −82.38°W), VEN (Cariaco Gulf, Venezuela; 10.48°N, −63.72°W).

Chamelecón.

2.7. Kingston Harbour (Jamaica, JAM)

Kingston Harbour is a bar-built estuary, which serves as the major port of Jamaica. The harbour is an elongated bay, extending 26 km of navigable water from east to west and 6.5 km from north to south, with a total surface area of approximately 51 km^2 (Wade, 1976) and with depths of up to 18 m. It is bordered by the city of Kingston (669,773 inhabitants in 2018; STATINJA, 2020); over 60,000 people live within 1 km of the harbour's shore (Webber et al., 2019) and sewage from 25% of the population is discharged into the harbor, with limited or no treatment. Water circulation is influenced by low tidal action, wind and freshwater inflows from major gullies and waterways. It has long flushing times, e.g. ~18 days for surface waters, and of several months at the inner harbor (Webber and Webber, 2003). The shape and configuration morphology of the bay has been strongly modified since middle 19th century. Its major fluvial inputs are Rio Cobre, Duhaney River and the Sandy Gully surface water drainage system. Kingston Harbour was reported to be eutrophic as far back as 1968, owing to the release of domestic and industrial wastes from the city of Kingston (Dunbar and Webber, 2003), and contaminated by massive soil erosion and run-off of agrochemicals from the largest and richest agricultural valleys across the Rio Cobre basin (Mansingh and Wilson, 1995).

2.8. Coatzacoalcos River Estuary (Mexico, MEX)

The Coatzacoalcos River is Mexico's third most important river by flow rate (28,679 hm^3 $year^{-1}$). Its lower basin hosts the industrial area of Minatitlan–Coatzacoalcos (one of the largest oil and petrochemical production centers of Mexico), the cargo port of Coatzacoalcos and mineral exploitation areas (e.g. salt, silica sands and sulfur). The region is a critical zone for ecologic regulation and environment protection since early 1990s, owing to the economic importance and environmental problems, including contamination by trace metals and petroleum hydrocarbons due to the discharges of untreated wastes and frequent oil spills (Paez-Osuna et al., 1986; Vazquez et al., 1991; Rosales-Hoz and Carranza-Edwards, 1998). Increasing trace element contamination in the Coatzacoalcos River discharge area has been related to the input of eroded soils from the catchment, promoted by the large industrial and urban development in the region, especially since the early 1980s (Ruiz-Fernández et al., 2012).

2.9. Bluefields Bay (Nicaragua, NIC)

Bluefields Bay is an estuarine lagoon system, catalogued as a Ramsar Site (#1138 since 2001). It has an extension of 176 km^2 and maximum depth of 4 m. Four rivers flow into the bay (Escondido, Caño Negro, Kukra, and Torsuani) although it is mainly influenced by the fluvial discharges of the Escondido River (mean yearly flow of 850 m^3 s^{-1}), carrying a high sediment load (1.4 a 22.3 kg m^{-3} per day) (Brenes et al., 2007). The bay sustains an important artisanal fishing activity (shrimp, fish, oysters and clam). Siltation is a major environmental problem of the bay, which increased from 5 (1970) to 42 (1998) mm $year^{-1}$, attributed to socio-economic development in the area and the occurrence of natural disasters (Dumailo, 2003). Bluefields bay is affected by erosion and wastewater discharges from diverse industrial activities (e.g. mining, tannery, milk processing) and human settlements along the Escondido River watershed (RSIS, 2020a).

2.10. Almirante Bay (Panama, PAN)

The Almirante Bay is a semi-enclosed lagoon system in Bocas del Toro Archipelago, Panama. It is connected to the Caribbean Sea, and has relatively clear and oligotrophic waters, which sustain well-developed coral reefs. It has a maximum depth of 32 m, and receives fluvial inputs from several small rivers and creeks, and sediment plumes from the rivers Sixaola and Changuinola, through the oceanic inlet Boca del Drago. The presence of reef barriers and mangrove forests considerably reduce the effect of wind and meteorological events during the hurricane season. Environmental concerns are increasing untreated wastewater discharges, promoted by rapid tourism and population growth in Bocas del Toro; inland erosion and agricultural runoff due to expansion of pasture lands and plantations of banana and teak; as well as heavy metal and hydrocarbon contamination, and alteration of the sedimentation patterns caused by dredging and shipping activities through the bay (D'Croz et al., 2005; Seemann et al., 2014).

2.11. Gulf of Cariaco (Venezuela, VEN)

The Gulf of Cariaco is a marginal basin, one of the most productive in the Caribbean Sea, owing to nutrient delivery by seasonal upwelling and numerous watercourses (notably the rivers Manzanares and Carinicuao). The Gulf of Cariaco is ~60 km long and ~15 km wide, has an extension of 642 km^2 and a maximum water depth of 85 m (Van Daele et al., 2011). Bottom water moves in the west-east direction along the south coast until El Saco, a shallow sediment deposition zone where mangrove forests dampen the movement of water and waves. It sustains commercially important fishery resources (e.g. sardine, spadefish and shrimp). It is contaminated by trace metals and hydrocarbons, owing to industrial and domestic wastewaters transported by rivers, and intense marine traffic (Márquez et al., 2005; Romero et al., 2013). Carinicuao River flows through ~170 km of important production areas and it is in the most seismic activity zone in Venezuela.

3. Methods

The IAEA - RLA/7/012 project organized a radiochronology experts meeting to prepare a methodological guide to ensure that the collection, processing and analysis of the sediment cores used in this study followed a standardized procedure (OIEA, 2020b).

3.1. Sampling

Sediment cores were collected by using a gravity corer UWITEC™ with a transparent liner (1 m long, 8.9 cm inner diameter) between 2008 and 2009 at coastal locations (Fig. 1). None of the cores presented laminations nor signs of sediment disturbance (e.g. sediment cracks or infaunal burrows). The cores were immediately transported to the counterpart laboratory, where they were extruded and subsampled at 1 cm intervals. The mass of each section was recorded before and after drying (most countries at ≤60 °C for at least 48 h, although in some countries samples were freeze-dried). Sediments were ground to powder by using porcelain mortar and pestle (except the aliquots used for grain size analysis). The samples were stored in polyethylene bags and shipped to previously assigned laboratories for further analysis. All concentrations and activities are expressed on a dry weight basis.

3.2. Laboratory analysis

^{210}Pb analyses were carried out at Servicio Académico de Fechado (ICML-UNAM, Mexico), Centro de Estudios Ambientales de Cienfuegos (CEAC-Cuba) and Radiometrics Laboratory (IAEA-EL, Monaco). $^{210}Pb_{tot}$ activities were measured through its daughter product ^{210}Po by alpha spectrometry, assuming secular equilibrium between the two isotopes (Ruiz-Fernández and Hillaire-Marcel., 2009). Also, gamma-ray spectrometry (HPGe well-detectors) was used to determine ^{226}Ra (through the ^{214}Pb gamma emission line of 352 keV) and ^{137}Cs (661.5 keV). Counting uncertainties were generally ≤6% for alpha spectrometry and ≤10% for gamma spectrometry. Replicate analyses (n = 12) of the standard reference material IAEA-300 (Radionuclides in Baltic Sea sediment) confirmed good agreement (within 2σ) for $^{210}Pb_{tot}$ and ^{137}Cs.

Loss on ignition was determined as a rough estimation of organic matter (OM) content by combusting sediments in a muffle furnace at 550 °C (LOI_{550}). Grain size distribution was assessed by using a Malvern laser diffraction equipment. Aluminum concentrations were analyzed with an X-ray fluorescence (XRF) system (Spectro X lab 2000, Spectro Analytical Instruments) at IAEA-EL, Monaco. Replicate analysis ($n = 6$) of the reference materials IAEA-158, IAEA-405 and IAEA-433 indicated good agreement between certified and analytical values for most elements, with accuracies above 90% and uncertainties below 8% for most of the elements determined.

3.3. Data treatment

3.3.1. Statistical analysis

Basic statistics were obtained for all dataset variables, and analysis of variance (ANOVA) with Tukey post-hoc test (95% confidence) was used to evaluate differences in the mean values of these variables among the sediment cores. Cluster analysis was performed to identify which geochemical variable (LOI_{550}, sand, silt, clay and Al) better explained the variation of radionuclide activities observed within the sampling sites.

3.3.2. ^{210}Pb chronology

Excess ^{210}Pb ($^{210}Pb_{ex}$) was determined by the difference between total ^{210}Pb ($^{210}Pb_{tot}$) and supported ^{210}Pb ($^{210}Pb_{sup}$) activities, estimated from gamma-spectrometry derived ^{226}Ra activities. Depending on the observed profiles, ^{210}Pb chronologies were computed either by the constant sedimentation constant flux model (CFCS; Krishnaswamy et al., 1971) or by the constant flux model (CF; Robbins and Edgington, 1978), following the methodology and spreadsheet in Sanchez-Cabeza and Ruiz-Fernández (2012). Uncertainties were usually ≤15% for age, MAR and SAR. The ^{137}Cs depth profiles were used to derive a stratigraphic marker to attempt the corroboration of the ^{210}Pb age models.

3.3.3. $^{210}Pb_{ex}$ and ^{137}Cs inventories

The radionuclide inventories were calculated by integrating over the core length the product of radionuclide activity (Bq kg^{-1}) and dry mass (kg) divided by the cross sectional area of the corer (Sanchez-Cabeza and Ruiz-Fernández, 2012). Radionuclide activities in unmeasured sections were interpolated *versus* mass depth (g cm^{-2}). Uncertainty was calculated by quadratic uncertainty propagation. Differences among cores were assessed through Student's *t*-test.

4. Results

4.1. Radionuclide spatial variability

Activities ranges were 4.5–259 Bq kg^{-1} for $^{210}Pb_{tot}$ and 4.5–50.6 Bq kg^{-1} for ^{226}Ra (Table 1, Fig. 2). Most cores showed $^{210}Pb_{tot}$ activities <100 Bq kg^{-1} (except CUB, HON, MEX and VEN) and ^{226}Ra activities < 20 Bq kg^{-1} (except COL, MEX and VEN). ^{137}Cs ranged from <LD (0.1 Bq kg^{-1}) to 7 Bq kg^{-1}, with lowest values (<2 Bq kg^{-1}) observed in COL, CUB and HAI. The inventories of $^{210}Pb_{ex}$ (Bq m^{-2}) ranged from 2965 ± 22 in PAN to 22,230 ± 609 in MEX, accounting for $^{210}Pb_{ex}$ fluxes between 92 ± 1 and 693 ± 19 Bq m^{-2} $year^{-1}$, respectively; whereas the ^{137}Cs inventories ranged from 47 ± 2 Bq m^{-2} $year^{-1}$ in HAI and 1,055 ± 54 Bq m^{-2} $year^{-1}$ in MEX (Table 1, Fig. 3). A cluster analysis was performed to evaluate the main source of variability of $^{210}Pb_{tot}$, ^{226}Ra and ^{137}Cs activities in the database (Fig. 4). Results showed two main groups (LOI_{550} and sand; silt, ^{226}Ra, $^{210}Pb_{tot}$, ^{137}Cs, Al and clay), and in the final partition, separate clusters were observed for i) $^{210}Pb_{tot}$, ^{137}Cs and Al, and ii) ^{226}Ra and silt.

4.2. ^{210}Pb chronologies and ^{137}Cs depth profiles

$^{210}Pb_{tot}$ depth profiles (Fig. 5) showed decreasing values downcore, but without clear exponential trends. The CF model was used to calculate all chronologies except for the MEX core, dated by using a 2 piecewise CFCS model because the presence of a $^{210}Pb_{ex}$ depleted segment, attributed to recent deposition of old sediments, excavated in the Coatzacoalcos river (Ruiz-Fernández et al., 2012). Most sediment records spanned ~100 years (Table 1S) except four younger cores COL, HON and JAM (owing to high sedimentation), as well as MEX (due to its short length).

^{137}Cs activities (Fig. 5) were detectable since the bottom sections of the younger cores COL (1973), HON (1947), JAM (1940) and MEX (1956), since the mid-1940s in cores PAN and VEN, and since the early 1990s in HAI, according to the ^{210}Pb-derived age models (Table 1S). Cores CUB, DOM, GUA and NIC showed detectable ^{137}Cs in sediments older than the first nuclear weapon test (1945, Trinity test). Only PAN and GUA showed a maximum that, according to the ^{210}Pb-age models, could be attributable to the ^{137}Cs global fallout maximum (1962–1964). All cores showed higher ^{137}Cs activities in the top segments.

4.3. Sediment accumulation

Mass accumulation rates (MAR) and sediment accumulation rates (SAR) varied widely among and within the cores (Fig. 6). Highest MAR was usually below 1 g cm^{-2} $year^{-1}$, and highest SAR was usually below 2 cm $year^{-1}$. MAR in cores COL, CUB and DOM, and SAR values in COL, CUB, DOM and JAM were significantly ($p < 0.05$) higher than the other cores (Fig. 6, Table 1). Both MAR and SAR showed steady increases in most cores, except CUB, DOM and HON, where clear maxima were observed at intermediate depths (up to 10 cm $year^{-1}$).

5. Discussion

5.1. Radionuclide spatial variability

The overall database showed an important variability of $^{210}Pb_{tot}$ and ^{226}Ra activities in the region (Fig. 2). Generally speaking, activities were low, with $^{210}Pb_{tot}$ activities in HON, MEX and VEN being significantly ($p < 0.05$) higher than in the rest of the cores, and highest values of ^{226}Ra were found in COL, MEX and VEN.

Activities of $^{210}Pb_{tot}$ in sediments are the result of ^{210}Pb fallout (in coastal sites mainly controlled by atmospheric ^{210}Pb concentrations and rainfall), *in situ* production owing to ^{222}Rn radioactive decay, and land surface runoff (mainly caused by fluvial inputs and watershed erosion). According to a simulated global distribution of monthly mean ^{210}Pb concentrations in surface air, and the latitudinal variation of the annual average total ^{210}Pb deposition fluxes (Liu et al., 2001), WCR is within a latitudinal band characterized by low atmospheric ^{210}Pb fluxes, very likely owing to a low ratio of the continent land mass/ocean area. The scarce data on ^{210}Pb fluxes in the WCR latitudes show values ranging from 133 ± 83 to 198 ± 112 Bq m^{-2} $year^{-1}$ for the latitudinal band 10–30°N (Baskaran, 2016). However, $^{210}Pb_{ex}$ deposition fluxes in most cores (Table 1; mean $^{210}Pb_{ex}$ flux of 284 ± 116 Bq m^{-2} $year^{-1}$) fell within the common range of $^{210}Pb_{ex}$ water-sediment deposition flux in coastal areas in the northern hemisphere (100–450 Bq m^{-2} $year^{-1}$; Preiss et al., 1996). These relatively high values were caused by the high contribution of erosion, mainly through river inputs, and some degree of fine sediment focusing at the sampling sites. The highest $^{210}Pb_{ex}$ fluxes were observed in HON and MEX (556 ± 5 and 693 ± 19 Bq m^{-2} $year^{-1}$, respectively), which were collected in coastal environments surrounded by extensive catchment areas and irrigated by large rivers: 21,336 km^2, 910 m^3 s^{-1} for the Coatzacoalcos River, Mexico (CONAGUA, 2018), and 3757 km^2, 370 m^3 s^{-1} for Chamelecon River, Honduras (USGS, 2002; Seeliger and Kjerfve, 2000).

^{226}Ra in soils is mostly associated to the natural abundance of ^{238}U of the parent rock mineralogical composition. During rock weathering (leaching and dissolution of minerals), ^{226}Ra can be solubilized in surface or ground waters, and transferred with the water flow until it

Table 1
Basic statistics of radionuclide data, Al concentrations, accumulation rates, ^{137}Cs inventories and $^{210}Pb_{ex}$ inventories and fluxes in sediment cores from the Wider Caribbean Region.

Variable	Core										
	COL	CUB	DOM	GUA	HAI	HON	JAM	MEX	NIC	PAN	VEN
$^{210}Pb_{tot}$ (Bq kg^{-1})											
N	36	35	47	18	14	37	31	26	48	53	60
Min	18.2	11.0	4.5	10.1	6.5	53.1	14.6	39.7	10.7	7.1	23.6
Max	54.7	259.0	56.5	92.1	40.5	184.5	49.2	114.0	61.8	69.6	201.0
Mean	36.5	41.3	21.4	44.4	26.0	134.7	32.3	67.0	39.4	37.8	96.3
SD	11.7	54.7	15.6	30.6	10.8	29.7	11.1	17.2	12.9	20.6	37.2
Median	35.9	24.7	14.5	44.8	29.8	131.2	37.6	64.5	41.2	38.1	96.7
^{226}Ra (Bq kg^{-1})											
N	36	35	47	18	15	37	31	26	48	11	60
Min	14.5	5.1	4.5	10.4	6.0	11.7	8.0	13.9	10.2	6.8	23.9
Max	28.1	14.1	7.6	13.1	11.6	11.7	15.0	27.0	14.4	8.0	50.6
Mean	22.0	8.5	5.9	11.8	9.1	11.7	12.1	20.4	12.1	7.4	40.6
SD	4.3	2.4	0.7	0.7	1.5	0.0	1.5	3.3	1.0	0.4	5.3
Median	23.3	8.1	5.9	12.0	9.5	11.7	12.4	21.2	12.2	7.5	39.9
$^{210}Pb_{ex}$ (Bq kg^{-1})											
N	36	8	36	12	7	36	30	26	45	49	23
Min	1.6	5.1	0.3	12.8	10.2	41.4	1.7	26.9	3.7	5.3	91.5
Max	30.2	19.1	50.2	86.1	28.7	176.6	37.5	100.8	39.7	58.1	193.4
Mean	14.4	9.4	18.9	55.4	19.8	127.0	21.0	54.1	24.5	30.4	123.4
SD	8.4	4.3	15.4	23.9	5.8	29.6	11.4	17.4	9.9	17.1	25.0
Median	13.7	8.0	17.9	60.1	18.5	122.7	26.6	53.0	24.5	30.2	117.4
^{137}Cs (Bq kg^{-1})											
N	27	21	47	18	15	37	31	26	48	20	20
Min	0.9	0.3	1.0	*	*	2.4	*	1.4	0.8	*	1.4
Max	1.9	1.6	3.0	7.0	1.1	4.7	4.1	3.9	3.8	2.6	3.5
Mean	1.2	1.1	1.9	4.5	0.4	3.8	2.1	2.4	2.5	1.6	2.4
SD	0.3	0.4	0.5	1.6	0.5	0.6	1.0	0.8	0.8	0.5	0.6
Median	1.2	1.1	1.8	5.0	*	3.9	1.8	2.3	2.7	1.6	2.4
Al (%)											
N	60	29	65	36	48	37	18	26	42	55	53
Min	1.1	4.7	4.2	4.3	1.3	8.6	2.8	4.5	6.0	3.5	8.9
Max	6.1	6.1	5.4	5.4	2.3	9.1	5.1	7.9	10.4	4.4	11.1
Mean	3.5	5.8	4.9	4.8	1.9	8.9	3.7	6.2	9.4	3.9	10.3
SD	1.2	0.3	0.3	0.3	0.3	0.1	0.8	0.9	0.8	0.2	0.5
Median	3.7	5.9	4.9	4.7	1.9	8.8	3.3	6.2	9.6	3.9	10.3
MAR (g cm^{-2} year^{-1})											
N	65	22	65	28	45	36	110	26	45	49	45
Min	0.6	0.4	0.03	0.03	0.03	0.3	0.3	0.7	0.03	0.01	0.1
Max	1.1	8.0	9.9	0.2	0.4	0.9	0.6	0.8	0.4	0.2	0.5
Mean	0.8	2.1	1.6	0.1	0.2	0.5	0.4	0.7	0.2	0.1	0.3
SD	0.1	1.6	2.3	0.1	0.1	0.2	0.1	0.1	0.1	0.0	0.1
Median	0.8	2.1	0.6	0.1	0.3	0.4	0.4	0.7	0.2	0.1	0.3
SAR (cm year^{-1})											
N	65	22	65	28	45	36	110	26	45	49	45
Min	1.3	0.6	0.1	0.1	0.04	0.3	0.9	0.4	0.04	0.04	0.1
Max	2.9	10.3	11.3	1.1	2.0	1.4	6.2	0.6	1.5	2.8	1.7
Mean	1.9	2.5	1.8	0.3	0.5	0.7	1.9	0.5	0.5	0.5	0.7
SD	0.3	2.0	2.3	0.2	0.4	0.3	1.1	0.1	0.4	0.5	0.4
Median	1.8	2.3	0.8	0.3	0.4	0.6	1.4	0.6	0.4	0.4	0.6
Radionuclide inventories (Bq m^{-2})											
$^{210}Pb_{ex}$	5807	7085	8908	5260	3890	17838	4621	22230	7302	2965	14328
±	148	214	257	37	89	169	51	610	195	22	406
^{137}Cs	360	169	1056	390	47	1050	823	905	615	100	393
±	12	13	28	9	4	27	13	54	14	2	18
Flux (Bq m^{-2} year^{-1})											
$^{210}Pb_{ex}$	181	221	278	164	121	556	144	693	228	92	447
±	5	7	8	1	3	5	2	19	6	1	13

NA = not available; *below minimum detectable activity (0.1 Bq kg^{-1}).

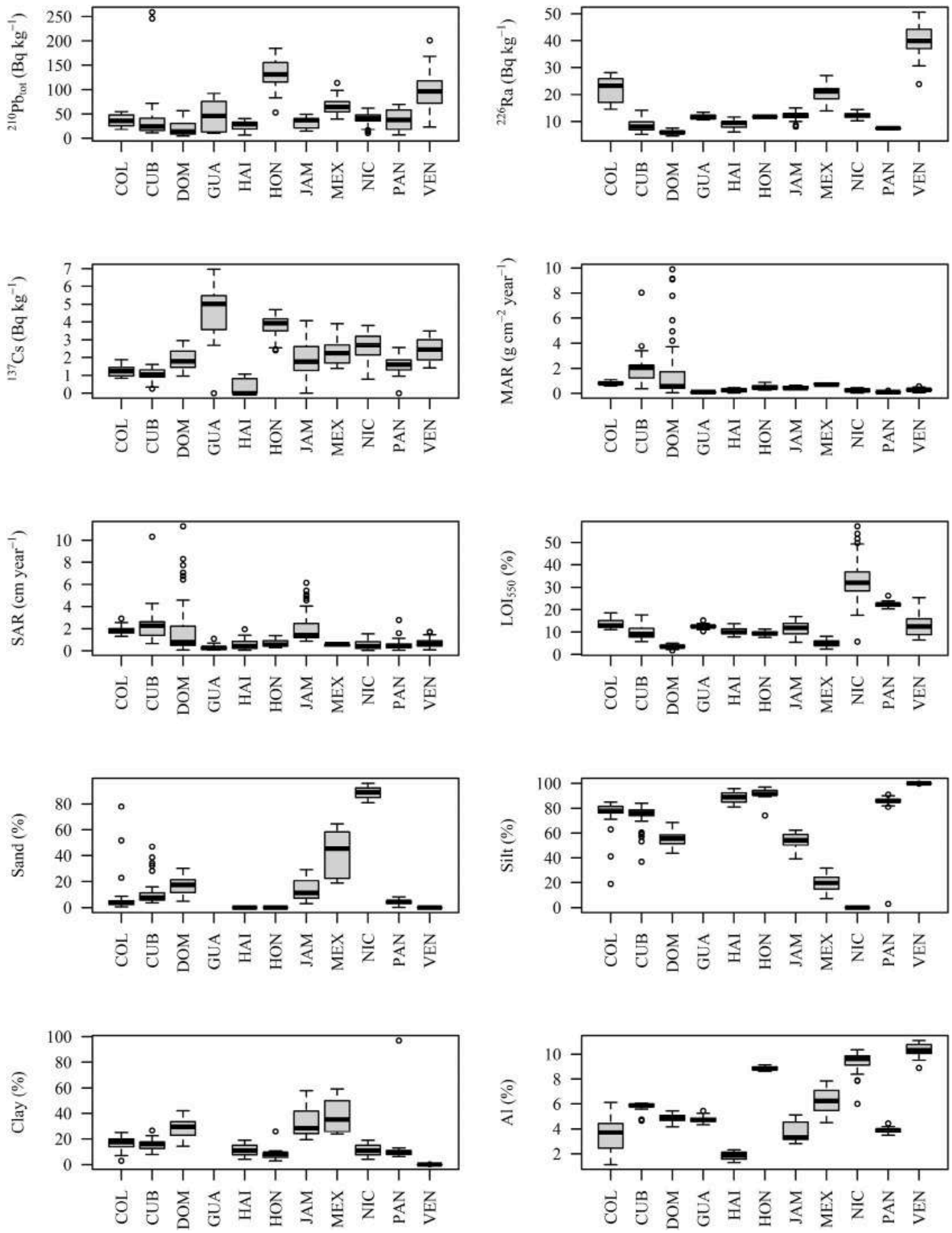

Fig. 2. Boxplot of radionuclide activities, Al concentrations and sedimentation rates in sediment cores collected from the Wider Caribbean Region.

becomes adsorbed onto suspended or settled particles. ^{226}Ra sorption is most effective by smaller grains, owing to a greater surface to volume ratio (Webster et al., 1995), by clays, metal hydroxides and humic substances, and under conditions of neutral to alkaline pH (Urso et al., 2019) and low salinities (IAEA, 1990). ^{226}Ra can also be enriched in soils owing to continued and long-term application of phosphate fertilizers (Khan et al., 2018). ^{226}Ra in marine sediments is mostly derived from local production by ^{230} Th day plus the fluvial contribution of soil particles.

The low ^{137}Cs activities are the result of low fallout in lower latitudes of the northern hemisphere (Aoyama et al., 2006), the time elapsed since ^{137}Cs fallout (~1963) and the high solubility of ^{137}Cs in seawater. According to UNSCEAR (2000), the 10°–20° N latitudinal band (where most of the sampling sites are located; Fig. 1) received ~11% of the total radionuclide deposition on the northern hemisphere from atmospheric nuclear testing. In addition, only ~65% the ^{137}Cs deposited in 1963 would remain in the environment, owing to radioactive decay, since no significant ^{137}Cs has been released in the region since 1960s. In addition, high ^{137}Cs solubility in seawater causes that >99% of ^{137}Cs in marine waters remains in solution (Molero et al., 1995 and references therein; Atwood, 2013) and, owing to ocean stratification, ^{137}Cs is not efficiently transported to bottom waters. In addition, ^{137}Cs can be transferred by runoff to the coastal zone were, owing to salinity changes, can be recycled and scavenged mostly by fine particles (e.g. organic matter and

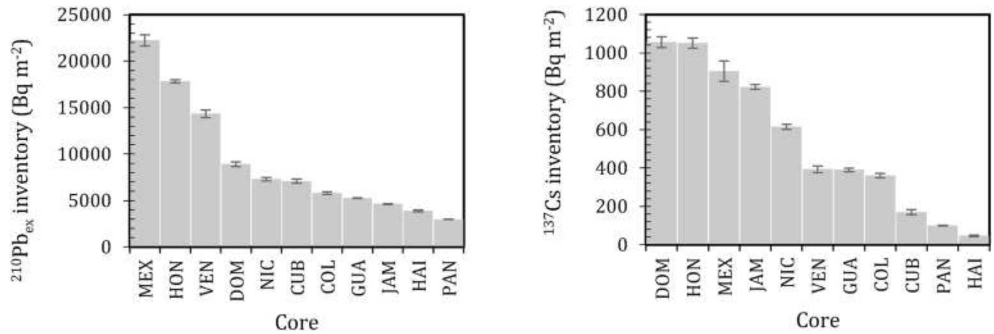

Fig. 3. Inventories of excess ^{210}Pb and ^{137}Cs in sediment cores from the Wider Caribbean Region.

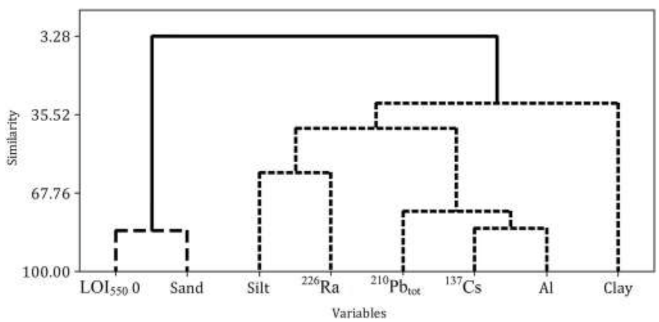

Fig. 4. Dendrogram from a cluster analysis of radionuclide activities and some geochemical variables in sediment cores from the Wider Caribbean Region.

clay minerals) to be finally deposited to the sediments.

Data on ^{137}Cs inventories in shallow coastal areas, influenced by fluvial inputs, in similar latitudes are scarce in the literature. The ^{137}Cs inventories (47 ± 2–1056 ± 54 Bq m^{-2}) were low in comparison with values reported for areas influenced by river discharges in the Adriatic Sea (up to 30,000 Bq m^{-2}; Papucci et al., 1996), where prodelta sediments seem to have a high trapping efficiency for fallout ^{137}Cs, but receive additional ^{137}Cs inputs through surface soils, eroded from the catchment, that were previously contaminated by ^{137}Cs fallout. The mean ^{137}Cs inventory in this study (537 ± 221 Bq m^{-2}) fell within the range reported for shallow nearshore sediments in NW Atlantic (144–544 Bq m^{-2}; Livingston and Bowen, 1979). The highest ^{137}Cs inventories observed in DOM, HON and MEX were comparable to values reported for Sagua Estuary (1160 ± 162 Bq m^{-2}) and undisturbed pasture fields near Cienfuegos Bay in Cuba (1200 ± 198 Bq m^{-2}, Díaz-Asencio et al., 2009 and references therein).

Cluster analysis showed that the main carrying phase of $^{210}Pb_{tot}$, ^{226}Ra and ^{137}Cs to sediments are fine grained particles. The clustering of $^{210}Pb_{tot}$ and ^{137}Cs activities with Al concentrations (as indicator of terrigenous input) and ^{226}Ra activities with silt-sized particles suggests that the main variability source of radionuclides is fluvial runoff to the study sites. Aluminosilicate particles are considered a primary phase carrying $^{210}Pb_{tot}$ from the water column to the sea floor in tropical areas (Legeleux et al., 1996) and it seems that, regionally speaking, ^{226}Ra is contained in minerals predominantly present in medium-sized (silt) particles.

5.2. ^{210}Pb chronologies and ^{137}Cs depth profiles

Most $^{210}Pb_{tot}$ depth profiles showed departures from the exponential decreasing trend, and these non-monotonic profiles could be indicative of post-depositional sediment mixing, since physical stirring due to strong erosive currents produced by winds and tides, as well as bioturbation, often result in obliterating the original ^{210}Pb signal. However, other processes can have similar effects on sediment records; for instance, reduced $^{210}Pb_{ex}$ activities at a core surface segment (e.g. cores GUA, JAM, NIC, PAN) could be the result of very rapid sedimentation (Appleby, 1998). As shown by Krishnaswamy et al. (1971), $^{210}Pb_{ex}$ activities in the sediments result from the balance between the $^{210}Pb_{ex}$ flux to the sediments and the sediment load (i.e. mass accumulation rate, MAR); this implies that $^{210}Pb_{ex}$ activities would decrease as a result of dilution by a higher MAR, or increase if the MAR was lower.

$^{210}Pb_{ex}$ profiles mostly shaped by radioactive decay would be only expected in environments where steady state sedimentation conditions prevail, but such conditions are hardly met in the coastal zone. Firstly, because of the multiplicity of particle sources and the highly variable sedimentation conditions that characterize the estuarine areas (UNESCO, 1978); and secondly, owing to the "Great Acceleration" of population growth and industrialization (Steffen et al., 2007) that characterizes the Anthropocene (i.e. from 1950 onwards; AWG, 2019). One of the most conspicuous evidences of global change is the increasing erosion owing to land use changes (Vitousek, 1994) and the increment in sediment accumulation rates in the coastal environments. Consequently, $^{210}Pb_{ex}$ profiles from anthropized areas in the dynamic coastal environment will seldom show an exponential decay trend. In this study, the deviations observed in the $^{210}Pb_{ex}$ profiles were interpreted as changes of sediment accumulation, under the assumption that post-depositional mixing was likely minor.

Independent validation of the chronology is essential for a high level of confidence in the dating results, for instance by using ^{137}Cs activity profiles as time stratigraphic markers (Smith, 2001). However, the ^{137}Cs stratigraphic profiles were of limited usefulness to corroborate ^{210}Pb-derived age models, owing to the lack of a clear ^{137}Cs activity maximum (except PAN and GUA). Other processes that might limit the effective use of the ^{137}Cs as stratigraphic marker in the coastal zone are the input by runoff and postdepositional remobilization. Fluvial input of ^{137}Cs-bearing soils eroded from the catchment could mask the expected global fallout maximum of ^{137}Cs in ~1963 and could also explain the relatively high ^{137}Cs activities observed in the recent core sections, in comparison to the older ones. Mobility problems for ^{137}Cs have also been recurrently reported since long ago (e.g. Davis et al., 1984; Carpenter, 1997; Klaminder et al., 2012; Wang et al., 2017). Some sediment components (clay minerals, organic matter, carbonates and iron-manganese oxy-hydroxides) are known to bind ^{137}Cs (Ashraf et al., 2014) and can be affected by burial diagenesis, which would promote the release and downward transport of ^{137}Cs in the pore waters through the sediment column, which could explain the presence of ^{137}Cs in layers presumably deposited before the onset of nuclear tests (such as in cores CUB, DOM, GUA and NIC). Higher salinities in the overlying water column and pore waters can produce ^{137}Cs desorption and upward migration, due to increasing competing ions such as sodium and potassium, whereas lower in the sediments, as the release of NH^{4+}, Fe^{2+} and Mn^{+2} in anaerobic conditions promotes the ion-exchange displacement of ^{137}Cs from sediments (Evans et al., 1983). Despite all these limitations, ^{137}Cs maxima were compatible with the chronologies obtained for PAN and GUA; and in addition, cores COL, HON, MEX and

Journal of Environmental Radioactivity 223–224 (2020) 106366

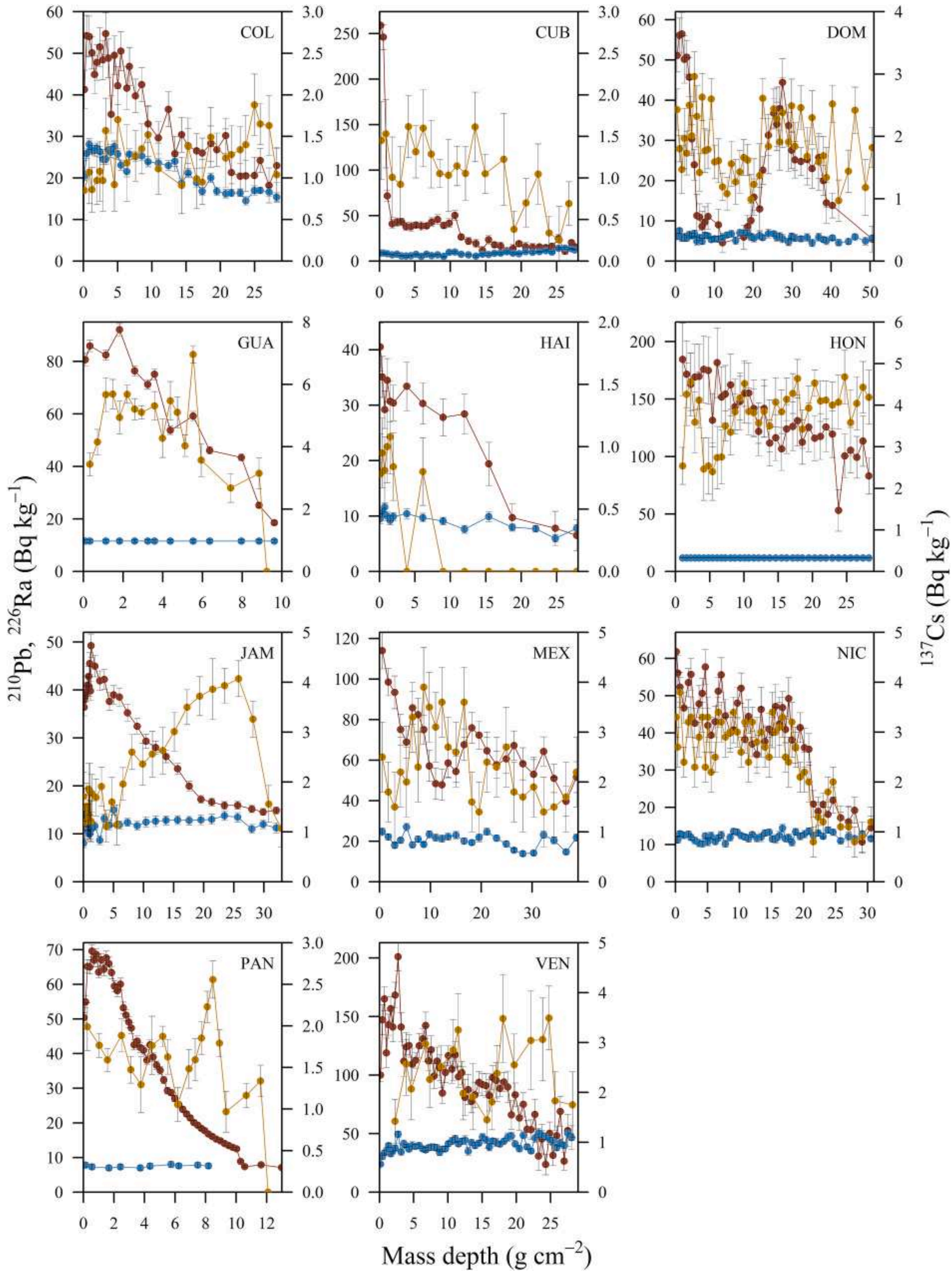

Fig. 5. Radionuclide activity (total ^{210}Pb, red; ^{226}Ra, blue; ^{137}Cs, yellow) depth profiles (mass depth) in sediment cores from the Wider Caribbean Region. (For interpretation of the references to colour in this figure legend, the reader is referred to the Web version of this article.)

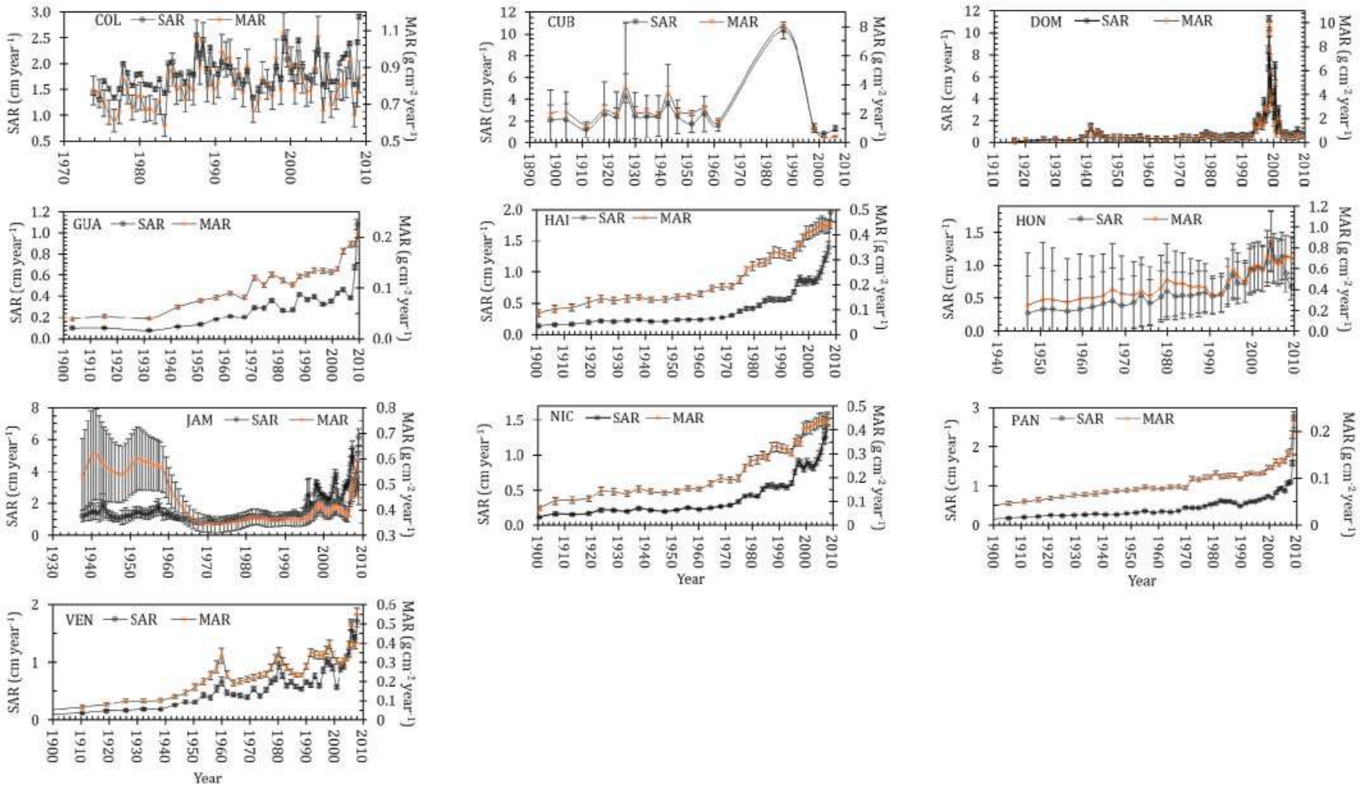

Fig. 6. Temporal variation of sediment accumulation rates (SAR) and mass accumulation rates (MAR) in sediment cores from the Wider Caribbean Region.

VEN showed ^{137}Cs activities in all sections, indicating that these sediments accumulated after the onset of the nuclear testing period, in agreement with the ^{210}Pb-derived dates.

Owing to all the problems to corroborate ^{210}Pb-derived chronologies with ^{137}Cs depth profiles, other stratigraphic markers are needed for low latitude coastal environments. Plutonium isotopes have lower post-depositional mobility than ^{137}Cs, for which their use as stratigraphic markers might be a good alternative (Hancock et al., 2011). Plutonium isotope depth profiles have been used to corroborate ^{210}Pb chronologies in coastal areas of Cuba and Mexico, including cores CUB (Diaz-Asencio et al., 2011; Corcho Alvarado et al., 2014) and MEX (Ruiz-Fernández et al., 2012). Furthermore, independent chronostratigraphic features in pollen, diatom or anthropogenic substances (e.g. heavy metals) might be used as time markers in recent sediments (UNESCO, 1978; Appleby, 1998). The cores COL, CUB and MEX have been previously used to study trace element contamination. High mercury concentrations recorded in core COL between 1970s and 1980s were related to the discharge of mercury contaminated wastes to Cartagena Bay from a chlor-alkali plant that used mercury as a cathode in the production of chlorine, and the maximum values in the late 1970s, and the subsequent decreasing concentrations, were related to the plant closure (Orani et al., 2020). In core CUB, the temporal variability of the anthropogenic fluxes of Pb, Zn, Sn, Hg and Cr accurately described the increasing impact from the urban and industrial activities around Havana Bay between the beginning of past century and 1980s; and the drastic reduction of these fluxes since 1990s was attributed to the combination of coastal zone management policies and the economic contraction of Cuba (Díaz-Asencio et al., 2011). In core MEX, concentrations of major (Al, Ca) and trace (Sr, Rb, As, Cu, Ni, V and Zn) elements showed a change of sediment and contamination sources since early 1980s, resulting from the large industrial and urban development in the Coatzacoalcos River discharge area, indicating that the increased contaminant loads were related to eroded soils from the catchment, due to extensive land use changes (Ruiz-Fernández et al., 2012). The data on plutonium isotope activities and heavy metals concentrations from these works can be found in the original sources.

In this work, efforts were made to corroborate the age models by combining the ^{137}Cs data with $^{210}Pb_{tot}$ stratigraphic features (Fig. 5) and MAR profiles (Fig. 6), based on historical data available at each site. Owing to the influence of changes in sediment density (due to compaction with time) SAR values must be taken with caution; MAR was preferred over SAR to explain these historical variations. ^{210}Pb chronologies proposed for most cores are only preliminary and may be adjusted in the future if additional information is available; further research on contamination in the cores might contribute to this purpose.

5.3. Colombia

MAR at Cartagena Bay was moderately variable (Table 1, Fig. 6). The main source of variability is apparently related to interventions in the Dique channel, through which most sediments enter the bay. The lowest values were recorded before early 1980s and the increments observed afterwards were attributed to the last rectification of the Dique channel (1975–1983), which increased 26% the water flow, and thus sediment delivery (UNC, 2007).

5.4. Cuba

MAR values were highly variable between 1910s and 1980s (Fig. 6), with maxima associated with the occurrence of extreme meteorological events in 1926 (the Great Hurricane), 1944 (Cuba–Florida hurricane) and 1982 (the heaviest rains reported in Havana over the 20th century). Since 1990, MAR values are similar to those observed in 1900, which were attributed to the reduction of economic activities in the entire catchment area between 1990 and 1995 (associated with the economic contraction of Cuba in the early 1990s due to the economic collapse of the socialist block), and with environmental measures implemented since 1998 to reduce the input of suspended solids to Havana Bay, which have contributed to restore natural sediment flows in this coastal ecosystem (Díaz-Asencio et al., 2011).

5.5. Dominican Republic

MAR values where almost constant (within the uncertainties) through the sediment record, and maxima are in close agreement with the occurrence of extreme events (e.g. San Cristobal storm in 1945; hurricane David and storm Frederick in 1978; Georges hurricane in 1998). The lower reach of Haina River is impacted by urban and industrial activities, sand extraction, deforestation and oil residues (Gómez Mena et al., 2008). However, excluding MAR maxima, the MAR range (from <0.06–0.8 cm $year^{-1}$) would place the port of Haina River among the areas least impacted by siltation in this study.

5.6. Guatemala

The MAR profile showed almost constant values between 1900s and early 1930s, a steady increase between early 1940s and 2000s (~2 fold within the period), which speeded up through the last decade of the record (~4 fold with respect to the values recorded in early 1940s). MAR increments were attributed to deforestation trends in the catchment area of Amatique Bay. The country has lost ~11% of its forest cover within 1991/93–2001 owing to the development of agriculture and cattle raising activities, the growth of disordered human settlements, and the occurrence of prolonged drought periods and forest fires (IARNA, 2006).

5.7. Haiti

In the Bay of Port-au-Prince, MAR values showed a steady increase throughout the record, albeit at a faster pace since 1970s. Deforestation is a pervasive environmental problem in Haiti since the beginning of the 19th century. Forest cover in Haiti has decreased from 60% in 1923 (Johnson Williams, 2011) to 30% in 1940, 10% in 1970 and to 4% in 2010 (FAO, 2010), and the primary forest has declined from 4.4% in 1988 to 0.32% in 2016 (Hedges et al., 2018). Accelerating deforestation and soil erosion since early 1950s is attributed to environmentally unsound agricultural practices, rapid population growth; and increasing logging operations since 1970s, owing to Port-au-Prince's intensified demand for charcoal (Johnson Williams, 2011).

5.8. Honduras

MAR values in HON were almost constant (within the uncertainties) along the core, and are relatively high in comparison with the rest of the cores. Forest cover loss in Honduras has been reported to be very high (~23% between 1958 and 1990, and ~30% between 1990 and 2005; FAO, 1960 and 2010) owing to extensive agriculture and logging activities and the development of human settlements. No remarkable feature in the MAR profile was observed, that could serve as a time marker to corroborate the ^{210}Pb-derived age model.

5.9. Jamaica

MAR values were almost constant and relatively high (0.58 ± 0.02 g cm^{-2} $year^{-1}$) between 1940 and the early 1960s, values declined sharply between 1960s and 1970s and were constant until middle 1990s, since when it showed a steady but rapid increase to reach a maximum comparable to values observed at the beginning of the record (0.59 ± 0.04 g cm^{-2} $year^{-1}$) in 2008. The declining MAR values recorded between 1960 and 1970 are most likely related with the construction of the Portmore Causeway (1968–1969), which was built to link Kingston with the Portmore development; however, before development began, about 800 ha of lowlands were filled by dredging the harbor, and a 19 km dyke structure was constructed to prevent flooding of the low-lying area from the Rio Cobre.

Environmental degradation of Kingston Bay has been recognized since late 1960s; the main impacts being eutrophication, sedimentation, and solid waste build-up, mostly related to urbanization and agricultural runoff. The harbor receives fresh water from two main rivers, a network of 19 major gullies that traverse the city and effluents from sewage treatment facilities. Sand mining, deforestation and poor farming practices lead to soil erosion in the river watersheds, promoting siltation; gullies carry solid wastes from residential and industrial areas, and sewage is the major cause of total suspended solids (Webber et al., 2019). Highest MAR values since the late 1990s might be related to i) the construction of Greater Portmore in the mid-1990s, which promoted a large population growth, ii) increasing upland erosion, as a result of large-scale agriculture since 1980s (mainly coffee plantations, FAO, 2003 and 2008), and iii) the occurrence of extreme events, which promote high sediment discharges, such as a flash flood in 1998, a flood in 2002, the hurricane Dean in 2007, and the tropical storms Nicole and Gustav in 2008. All these events are well represented as maxima in the MAR profile.

5.10. Mexico

The sediment record from the Coatzacoalcos river estuary spanned 52 years. The $^{210}Pb_{ex}$ profile showed a strong discontinuity between 9 and 14 cm depth, which was attributed to the accumulation of old sediments (depleted in $^{210}Pb_{ex}$). According to the ^{210}Pb-derived age model, the core section at the base of this discontinuity corresponded to 1984 ± 6, and it was related to deep excavations (2 m diameter and up to 13m depth) in the riverbed during the construction of a bridge at the lower reach of the Coatzacoalcos River in 1980, in agreement with the ^{210}Pb chronology (Ruiz-Fernández et al., 2012). Despite extensive land use changes and industrial development in the study area along the period comprised in the sediment record, the mean MAR values below (0.80 ± 0.08 cm $year^{-1}$, 1956–1982) and above (0.69 ± 0.16 cm $year^{-1}$, 1994–2008) the discontinuity were comparable, likely due to the high flow rate of the Coatzacoalcos River, which washes out and redistribute the eroded soils transported from the catchment.

5.11. Nicaragua

MAR values progressively increased over time, although the pace observed since the late 1970s was higher than in the previous decades. The small MAR maximum in 1987 ± 1 was attributed to higher sedimentation loads promoted by rainfall occurred during hurricane Joan in 1988. One of the main environmental problems in Bluefields Bay, increased siltation attributed to the land erosion from the catchment of Escondido River, is clearly observed in the MAR profile, especially since late 1970s. Similar findings were reported from the study of a sediment core collected in the lower reach of Escondido River (Dumailo, 2003), the main tributary of Bluefields Lagoon. The increasing accumulation rates were associated to deforestation in the Escondido River catchment, owing to extensive cattle raising, expansion of the agricultural frontier, recurrent forest fires and the proliferation of dirt roads.

5.12. Panama

MAR values steadily increased over time in Almirante Bay, most likely as a result of population growth and consequent human impacts, at a low pace since the beginning of the 20th century to 1970s, when agriculture was the most important economic activity in the region, and at higher pace since 1980s, owing to the fast development of tourism activities. The MAR maximum observed at the end of the profile was related to the occurrence of an intense rainfall occurred in November 2008.

5.13. Venezuela

MAR values showed a steady increase since the beginning of the record, with episodic maxima (e.g. 1960, 1980) and minima (1988 and 2002) for which we do not have a clear explanation. The continuous MAR increments can be explained by the periods i) 1940–1970s, with the development of the sardine industry, ii) 1970s–2000s, as after the nationalization of the oil industry, extensive country-wide LUC took place, and iii) a steeper pace since 2000, with the reactivation of the cocoa cultivation and export activities, which currently accounts for the 90% of Venezuelan exports. A similar MAR temporal profile was reported by Yang et al. (2016) for Jiaozhou Bay, China, where the temporal sedimentation dynamics was explained to be driven by changes in economic policies, in response to population and industry expansion.

6. Concluding remark

Although with different intensity, most sediment cores showed the impact of global change through the Anthropocene (since middle 1950s), evidencing increasing sediment and mass accumulation rates with time. Despite MAR ranges in cores GUA, HAI, NIC, PAN and VEN were among the lowest in this study (Table 1), it was remarkable that the values observed within the last decade implied between ~8 and ~21 fold increments in comparison with values recorded at the beginning of the century. Increasing rates were mostly attributed to continental erosion, likely associated with LUC in the catchment areas, for reasons specific to national development realities.

7. Conclusions

A survey on temporal variations of sediment accumulation within the past 100 years was performed in 11 countries of the Wider Caribbean Region. This information is the first-ever comprehensive study on this subject in the region. Although ^{210}Pb dating is a powerful tool to provide retrospective information on environmental changes in coastal environments, this study confirmed that corroboration of ^{210}Pb chronologies with ^{137}Cs was difficult, owing to the input of land eroded ^{137}Cs-enriched sediments, and to the low activities observed, which were caused by low ^{137}Cs global fallout in the region, high solubility of ^{137}Cs in seawater and radioactivity decay since the period of nuclear atmospheric testing. Thus, it is important to find alternative ways to corroborate the ^{210}Pb age models, including other radioactive methods, or historical information that could explain features of either ^{210}Pb profiles or derived mass accumulation rates, as shown in this survey.

Siltation is a common problem in all studied sites, and sedimentation rates have been steadily rising since the beginning of 20th century because of deforestation and soil erosion in the surrounding catchment areas, and poor management of urban and industrial wastes. Owing to the different characteristics of the study sites (from coastal lagoons to open waters), accumulation rates cannot be extrapolated and must be obtained for each area of interest. Retrospective studies based on ^{210}Pb dating are useful not only to evaluate the historical changes occurred in the coastal environments, but also to verify the usefulness of management programs to control the land-derived erosion and improve siltation problems, such as in Havana Bay (Cuba).

The results of this research must be taken with caution because (a) they stem from a single core per study site, which may not depict the conditions of the whole ecosystem; and (b) due to the lack of unequivocal validation of some ^{210}Pb chronologies. However, they are valuable because of the scarcity of environmental data at some of these sites, and lead to important conclusions regarding the coastal ecosystems in WCR. It is certainly expected that these preliminary results will promote further research on the interactions between anthropogenic activities and coastal environments in this region. Owing to the detrimental potential of siltation to the valuable coastal resources, it is strongly recommended to follow up on these retrospective evaluations, and to extend them to other areas, to assist integrated coastal zone management programs in the region and elsewhere.

Declaration of competing interest

The authors declare that they have no known competing financial interests or personal relationships that could have appeared to influence the work reported in this paper.

Acknowledgments

This study was supported by the IAEA Technical Cooperation projects RLA/7/012 and RLA/7/022. The authors are indebted to the experts that contributed to design the work strategy of this study, and the numerous scientists, technicians and students that contributed to core sampling and processing tasks. MEX core was collected thanks to the outstanding work of crew and scientists aboard the R/V "Justo Sierra" during GEOCRON-I campaign.

Appendix A. Supplementary data

Supplementary data to this article can be found online at https://doi.org/10.1016/j.jenvrad.2020.106366.

References

Andrade, H., Santos, J., Ixquiac, M.J., 2015. Ecological linkages in a Caribbean estuary bay. Mar. Ecol. Prog. Ser. 533, 29–46.
Angerville, R., Joseph, O., Emmanuel, E., Perrodin, Y., 2005. Ecological Risk Assessment of Heavy Metals in Paint Manufacturing Effluents of Port-Au-Prince. The Raison D'être of Environmental Toxicology and Chemistry. SETAC Europe Office, Brussels. Abstract book SETAC Europe 15th Annual Meeting, May 22-26 2005.
Aoyama, M., Hirose, K., Igarashi, Y., 2006. Re-construction and updating our understanding on the global weapons tests 137Cs fallout. J. Environ. Monit. 8, 431–438.
Appleby, P.G., 1998. Dating recent sediments by 210Pb: problems and solutions. In: Ilus, E. (Ed.), Dating of Sediments and Determination of Sedimentation Rate. Proceedings of a Seminar Held in Helsinki 2-3 April 1997. STUK-A145. Radiation and Nuclear Safety Authority, Helsinki, pp. 7–24.
Armenteros, M., Pérez-Angulo, A., Regadera, R., Beltrán, J., Vincx, M., Decraemer, W., 2009. Effects of chronic and heavy pollution on macro- and meiobenthos of Havana Bay, Cuba. Rev. Investig. Mar. 30 (3), 203–214.
Ashraf, M.A., Akib, S., Maah, M.J., Yusoff, I., Balkhair, K.S., 2014. Cesium-137: radiochemistry, fate, and transport, remediation, and future concerns. Crit. Rev. Environ. Sci. Technol. 44, 1740–1793.
Atwood, D.A., 2013. Radionuclides in the Environment. John Wiley & Sons, United Kingdom, p. 560.
AWG, 2019. Subcommission on Quaternary Stratigraphy. What is the Anthropocene? – current definition and status. Anthropocene Working Group the. http://quaternary.stratigraphy.org/working-groups/anthropocene/. Consulted: 30/03/2020.
Baskaran, M., 2016. Radon: A Tracer for Geological, Geophysical and Geochemical Studies. Springer, Switzerland, p. 260.
Boske, L.B., 2001. Maritime transportation in Latin America and the Caribbean project. A report by the policy research project on multimodal/intermodal transportation. http://ctr.utexas.edu/wp-content/uploads/pubs/PRP_138.pdf. Consulted: 18/05/2020.
Brenes, C.L., Hernández, A., Ballestero, D., 2007. Flushing time in Perlas lagoon and Bluefields bay, Nicaragua. Invest. Mar. 35 (1), 89–96.
Carpenter, R., 1997. Interactions of radionuclides with sediments and suspended particles. In: Strategies and Methodologies for Applied Marine Radioactivity Studies. International Atomic Energy Agency, Vienna, pp. 83–103. Sraining course series No.7.
Colantonio, A., Potter, R.B., 2006. City profile Havana. Cities 23, 63–78.
CONAGUA, 2018. Estadísticas del agua en México. Comisión Nacional del Agua, Secretaría de Medio Ambiente y Recursos Naturales. Ciudad de México, p. 303.
Corcho-Alvarado, J.A., Diaz-Asencio, M., Froidevaux, P., Bochud, F., Alonso-Hernández, C.M., Sanchez-Cabeza, J.A., 2014. Dating young Holocene coastal sediments in tropical regions: use of fallout 239,240Pu as alternative chronostratigraphic marker. Quat. Geochronol. 22, 1–10.
Cuellar-Martínez, T., Ruiz-Fernández, A.C., Sanchez-Cabeza, J.A., Alonso-Rodríguez, R., 2017. Sedimentary record of recent climate impacts on an insular coastal lagoon in the Gulf of California. Quat. Sci. Rev. 160, 138–149.
Davis, R.B., Hess, T., Norton, S.A., Hanson, D.W., Hoagland, K.D., Anderson, D.S., 1984. 137Cs and 210Pb dating of sediments from soft-water lakes in New England (U.S.A.) and Scandinavia, a failure of 137Cs dating. Chem. Geol. 44 (1–3), 151–185.
Díaz-Asencio, M., Alonso-Hernández, C.M., Bolaños-Álvarez, Y., Gómez-Batista, M., Pinto, V., Morabito, R., Hernández-Albernas, J.I., Eriksson, M., Sanchez-Cabeza, J.A.,

2009. One century sedimentary record of Hg and Pb pollution in the Sagua Estuary (Cuba) derived from 210Pb and 137Cs chronology. Mar. Pollut. Bull. 59, 108–115.
Díaz-Asencio, M., Corcho-Alvarado, J.A., Alonso-Hernández, C., Quejido-Cabezas, A., Ruiz-Fernández, A.C., Sanchez-Sanchez, M., Gómez-Mancebo, M.B., Froidevaux, P., Sanchez-Cabeza, J.A., 2011. Reconstruction of metal pollution and recent sedimentation processes in Havana Bay (Cuba): A tool for coastal ecosystem management. J. Hazard. Mater. 196, 402–411.
Dumailo, S., 2003. Assessment of the environmental problems in the Bluefields lagoon, RAAS, Nicaragua studying some aspects of sedimentation and contamination. UNAN-Nicaragua. https://repositorio.unan.edu.ni/2286/. Consulted: 20/03/2020.
Dunbar, F.N., Webber, M.K., 2003. Zooplankton distribution in the eutrophic Kingston Harbour, Jamaica. Bull. Mar. Sci. 73 (2), 343–359.
D'Croz, L., del Rosario, J.B., Góndola, P., 2005. The effect of fresh water runoff on the distribution of dissolved inorganic nutrients and plankton in the Bocas del Toro Archipelago, Caribbean Panama. Caribb. J. Sci. 41 (3), 414–429.
Emmanuel, E., Azaël, A., 1998. Les eaux usées et le développement économique en Haïti : crises et réponses. In: Zebidi (Ed.), Actes de la Conférence Internationale de l'UNESCO 3-6 juin 1998 « l'eau : une crise imminente, UNESCO PHI, vol. 18. Technical Documents in Hydrology, pp. 279–285.
ERH, 2019. Haiti at a glance. Embassy of the Republic of Haiti, Washington DC. https://www.haiti.org/haiti-at-a-glance/. Consulted: 15/03/2020.
Evans, D.W., Alberts, J.J., Clark, R.A.I.I.I., 1983. Reversible ion-exchange fixation of cesium-137 leading to mobilization from reservoir sediments. Geochem. Cosmochim. Acta 47, 1041–1049.
FAO, 1960. World forest inventory. Food and Agriculture Organization of the United Nations, Rome, p. 137.
FAO, 2003. WTO Agreement on Agriculture: the Implementation Experience - Developing Country Case Studies. Commodity Policy and Projections Service Commodities and Trade Division. Food and Agriculture Organization of the United Nations, Rome.
FAO, 2008. Jamaica: Country Report to the FAO International Technical Conference on Plant Genetic Resources for Food and Agriculture (2008). Food and Agriculture Organization of the United Nations, Kingston, p. 59.
FAO, 2010. Global Forest Resources Assessment 2010. Main Report. Food and Agriculture Organization of the United Nations, Rome, p. 340. FAO Forestry Paper 163.
Fonseca, E.A.C., Arrivillaga, A., 2003. Coral reefs of Guatemala. In: Cortés, J. (Ed.), Latin American Coral Reefs. Elsevier Science, Amsterdam, pp. 159–169.
Gómez Mena, J., Julia Mera, E., Meyreles, L., Portorreal, F., 2008. Natural and Social History of the Haina River. First part: natural and physical features of the Haina basin. Ciencia Soc. 33 (4), 475–494.
Hancock, G.J., Leslie, C., Everett, S.E., Tims, S.G., Brunskill, G.J., Haese, R., 2011. Plutonium as a chronomarker in Australian and New Zealand sediments: a comparison with 137Cs. J. Environ. Radioact. 102, 919–929.
Hedges, S.B., Cohen, W.B., Timyan, J., Yange, Z., 2018. Haiti's biodiversity threatened by nearly complete loss of primary forest. Proc. Natl. Acad. Sci. Unit. States Am. 115 (46), 11850–11855.
Herrera-Moreno, A., Betancourt, L., Alcolado, P., 2009. Impacto de la contaminación sobre los arrecifes coralinos al Oeste del Río Haina, San Cristóbal, República Dominicana. Reporte del Proyecto EcoMar: Impactos a los arrecifes dominicanos. Programa EcoMar en República Dominicana. https://programaecomar.com/. Consulted: 18/05/2020.
HIT, 2020. Rio Haina Port Handbook. Haina International Terminals. https://hit.com.do/wp-content/uploads/2019/12/DOHAI-PORT-HANDBOOK.pdf.
IAEA, 1990. The Environmental Behavior of Radium, vol. 1. International Atomic Energy Agency, Vienna, p. 599. Technical Reports Series No. 310.
IARNA, 2006. Perfil ambiental de la Republica de Guatemala. Instituto de Agricultura, Recursos Naturales y Ambiente, Universidad Rafael Landivar y Asociación Instituto de Incidencia Ambiental, Guatemala, p. 249.
INE, 2018. Puerto Cortés, Cortés. Información general/2018. Instituto Nacional de Estadística. https://www.ine.gob.hn/V3/imag-doc/2019/08/Puerto-cortes-cortes-2018.pdf. Consulted: 2020/03/23.
IOC/UNESCO, IMO, FAO, UNDP, 2011. A Blueprint for Ocean and Coastal Sustainability. IOC/UNESCO, Paris, p. 42.
ITT, 1985. Informe Final Proyecto CUB/80/001 Investigación y Control de la Contaminación Marina en la Bahía de la Habana. Instituto de Investigaciones del Transporte, PNUMA, UNESCO, p. 682 (in Spanish).
Johnson Williams, V., 2011. A case study of desertification in Haiti. J. Sustain. Dev. 4 (3), 20–31.
Khan, M.N., Mobin, M., Abbas, Z.K., Alamri, S.A., 2018. Fertilizers and their contaminants in soils, surface and groundwater. In: DellaSala, Dominick A., Goldstein, Michael I. (Eds.), The Encyclopedia of the Anthropocene, vol. 5, pp. 225–240.
Klaminder, J., Appleby, P., Crook, P., Renberg, I., 2012. Post-deposition diffusion of 137Cs in lake sediment: Implications for radiocaesium dating. Sedimentology 59 (7), 2259–2267.
Krishnaswamy, S., Lal, D., Martin, J., Meybeck, M., 1971. Geochronology of lake sediments. Earth Planet Sci. Lett. 11, 407–414.
Lefranc, A., 2016. Évaluation des risques écotoxicologiques des métaux lourds contenus dans les effluents urbains sur la baie de Port-au-Prince. Institut des Sciences, des Technologies et des Etudes Avancées d'Haïti, p. 75.
Legeleux, F., Reyss, J.L., Etcheber, H., Khripounoff, A., 1996. Fluxes and balance of 210Pb in the tropical northeast Atlantic. Deep Sea Res. Oceanogr. Res. Pap. 43 (8), 1321–1341.
Liu, H., Jacob, D.J., Bey, I., Yantosca, R.M., 2001. Constraints from 210Pb and 7Be on wet deposition and transport in a global three-dimensional chemical tracer model driven by assimilated meteorological fields. J. Geophys. Res. 106 (D11), 12109–12128.
Livingston, H.D., Bowen, V.T., 1979. Pu and 137Cs in coastal sediments. Earth Planet Sci. Lett. 43, 29–45.
Mansingh, A., Wilson, A., 1995. Insecticide contamination of Jamaican environment III. Baseline studies on the status of insecticidal pollution of Kingston Harbour. Mar. Pollut. Bull. 30 (10), 640–645.
Márquez, A., Bonilla, J., Martínez, G., Senior, W., Aguilera, D., González, A., 2005. Estudio geoquimico de los sedimentos superficiales del litoral nororiental del Golfo de Cariaco, Estado Sucre, Venezuela. Boletín del Instituto Oceanográfico de Venezuela, Universidad de Oriente 44 (2), 89–103.
MMARN, 2020. Haina. Ministerio de Medio Ambiente y Recursos Naturales. https://ambiente.gob.do/cuencas-hidrograficas/haina/. Consulted: 18/05/2020.
Molares, R., Mestres, M., 2012. Effects of fluctuating river discharge on the water exchange mechanism of a semi-enclosed micro-tidal bay: Cartagena Bay, Colombia. Boletín Científico del CIOH 30, 53–74.
Molero, J., Sanchez-Cabeza, J.A., Merino, J., Pujol, L.L., Mitchell, P., Vidal-Quadras, A., 1995. Vertical distribution of radiocaesium, plutonium and americium in the Catalan Sea (Northwestern Mediterranean). J. Environ. Radioact. 26, 205–216.
Noel, G.L., 1999. An Analysis of the Economic and Social Issues Associated with Restructuring the Port of Port-Au-Prince (Haiti), vol. 60. World Maritime University Dissertations, p. 75.
OIEA, 2020a. In: Sanchez-Cabeza, J.A., Alonso-Hernández, C., Ruiz-Fernández, A.C. (Eds.), Reconstrucción de la historia de la contaminación de las costas del Gran Caribe. Laboratorios del Medio Ambiente, Organismo Internacional de Energía Atómica. Mónaco, Monaco, p. 258. In press.
OIEA, 2020b. In: Ruiz-Fernández, A.C., Sanchez-Cabeza, J.A. (Eds.), Guía para el uso de sedimentos en la reconstrucción histórica de la contaminación en zonas costeras. Organismo Internacional de Energía Atómica, Monaco, p. 113. In press.
ONEI, 2017. Anuario Estadístico de Cuba 2016. Oficina Nacional de Estadística e Información. Habana, p. 447.
Orani A.M., Vassileva E., Azemard S., Alonso-Hernandez C. Trace elements contamination assessment in marine sediments from different regions of the Caribbean Sea. J. Hazard Mater. 399, 122934.
Páez-Osuna, F., Botello, A.V., Villanueva, S., 1986. Heavy metals in Coatzacoalcos Estuary and Ostion Lagoon, México. Mar. Pollut. Bull. 1711, 516–519.
Pagliardini, J., Gómez, M., Gutierrez, H., Zapata, S., Jurado, A., Garay, J., Vernette, G., 1982. Síntesis del Proyecto Bahía de Cartagena. Boletín Cientifico del CIOH 4, 49–110.
Papucci, C., Charmasson, S., Delfanti, R., Gascó, C., Mitchell, P., Sanchez-Cabeza, J.A., 1996. Time evolution and Levels of Man-Made Radioactivity in the Mediterranean Sea. In: Guéguéniat, P., Germain, P., Métivier, H. (Eds.), Radionuclides in the Oceans, vol. 177-197, ISBN 2-86883-285-7. Les Éditions de Physique, Les Ulis (France).
PNUMA, 2020. Wider Caribbean. Programa de Naciones Unidad para el Medio Ambiente. https://www.unenvironment.org/es/node/974. Consulted: 15/01/2020.
Preiss, N., Melières, M.A., Pourchet, M., 1996. A compilation of data on lead 210 concentration in surface air and fluxes at the air-surface and water-sediment interfaces. J. Geophys. Res. 101, 28,847–28,862. D22.
REMARCO, 2020. Red de Investigación Marino-Costera. http://remarco.cl.
Robbins, J.A., Edgington, D.N., 1975. Determination of recent sedimentation rates in Lake Michigan using Pb-210 and Cs-137. Geochem. Cosmochim. Acta 39, 285–304.
Romero, D., Martínez, G., Brito, F., Rodríguez, E., 2013. Estudio de línea base en la determinación de hidrocarburos aromáticos policíclicos totales en sedimentos superficiales del sector oriental del Golfo de Cariaco, Venezuela. Avances en Química 8 (1), 47–54.
Rosales-Hoz, L., Carranza-Edwards, A., 1998. Heavy metals in sediments from Coatzacoalcos River, Mexico. Bull. Environ. Contam. Toxicol. 60, 553–561.
RSIS, 2020a. Sistema de Humedales de la Bahía de Bluefields. Ramsar Sites Information Services. https://rsis.ramsar.org/ris/1139. Consulted: 29/02/2020.
RSIS, 2020b. Punta de Manabique. Ramsar Sites Information Service. https://rsis.ramsar.org/ris/1016?language=en. Consulted: 18/05/2020.
Ruiz-Fernández, A.C., Hillaire-Marcel, C., 2009. 210Pb-derived ages for the reconstruction of terrestrial contaminant history into the Mexican Pacific coast: Potential and limitations. Mar. Pollut. Bull. 59, 134–145.
Ruiz-Fernández, A.C., Sanchez-Cabeza, J.A., Alonso-Hernández, C., Martínez-Herrera, V., Pérez-Bernal, L.H., Preda, M., Hillaire-Marcel, C., Gastaud, J., Quejido-Cabezas, A.J., 2012. Effects of land use change and sediment mobilization on coastal contamination (Coatzacoalcos River, Mexico). Continent. Shelf Res. 37, 57–65.
Ruiz-Fernández, A.C., Maanan, M., Sanchez-Cabeza, J.A., Pérez Bernal, L.H., López Mendoza, P., Limoges, A., 2014. Cronología de la sedimentación reciente y características geoquímicas de sedimentos de la laguna de Alvarado, Veracruz (Golfo de México). Cienc. Mar. 40 (4), 291–303.
Ruiz-Fernández, A.C., Betancourt Portela, J.M., Sericano, J.L., Sanchez-Cabeza, J.A., Espinosa, L.F., Cardoso-Mohedano, G., Pérez-Bernal, L.H., Garay Tinoco, J.A., 2016. Coexisting sea-based and land-based sources of contamination by PAHs in the continental shelf sediments of Coatzacoalcos River discharge area (Gulf of Mexico). Chemosphere 144, 591–598.
Sanchez-Cabeza, J.A., Ruiz-Fernández, A.C., 2012. 210Pb sediment radiochronology: An integrated formulation and classification of dating models. Geochem. Cosmochim. Acta 82, 183–200.
Seeliger, U., Kjerfve, B., 2000. Coastal Marine Ecosystems of Latin America. Springer, Berlin, p. 366.
Seemann, J., González, C.T., Carballo-Bolaños, R., Berry, K., Heiss, G.A., Struck, U., Leinfelder, R.R., 2014. Assessing the ecological effects of human impacts on coral reefs in Bocas del Toro, Panama. Environ. Monit. Assess. 186, 1747–1763.

Smith, J.N., 2001. Why should we believe 210Pb sediment geochronologies? J. Environ. Radioact. 55 (2), 121–123.
STATINJA, 2020. Population statistics. Statistical Institute of Jamaica, 2020. https://statinja.gov.jm/Demo_SocialStats/PopulationStats.aspx. Consulted: 24/03/2020.
Steffen, W., Crutzen, P.J., McNeill, J.R., 2007. The Anthropocene: Are Humans Now Overwhelming the Great Forces of Nature. AMBIO A J. Hum. Environ. 36 (8), 614–621.
Tosic, M., Restrepo, J.D., Lonin, S., Izquierdo, A., Martins, F., 2019. Water and sediment quality in Cartagena Bay, Colombia: Seasonal variability and potential impacts of pollution. Estuar. Coast Shelf Sci. 216, 187–203.
UNC, 2007. Estudios e investigaciones de las obras de restauración ambiental y de navegación del canal del Dique. Estudio de sedimentos en el canal del Dique y su efecto en la Bahía de Cartagena. Universidad Nacional de Colombia. Bogotá, p. 97. Informe CM-CD-2.
UNEP, 1999. Assessment of Land-based Sources and Activities Affecting the Marine. In: Coastal and Associated Freshwater Environment in the Wider Caribbean Region, UNEP Regional Seas Reports and Studies 172. United Nations Environment Programme, p. 121.
UNEP, 2010. GEO Haiti. State of the Environment Report 2010. United Nations Environment Program. UNEP, Port-au-Prince, p. 187.
UNESCO, 1978. Biogeochemistry of estuarine sediments. In: Proceedings of a UNESCO/SCOR Workshop Held in Melreux, Belgium 29 November to 3 December 1976. United Nations Educational, Scientific and Cultural Organization, Paris, p. 293.
UNSCEAR, 2000. Sources and effects of ionizing radiation. In: United Nations Scientific Committee on the Effects of Atomic Radiation. United Nations, New York, p. 654. Report to the General Assembly, with Scientific Annexes. Volume I: Sources.
Urso, L., Hormann, V., Diener, A., Achatz, M., 2019. Modelling partition coefficients of radium in soils. Appl. Geochem. 105, 78–86.
USGS, 2002. Flood-Hazard Mapping in Honduras in Response to Hurricane Mitch. Water-Resources Investigations Report 01-4277. U.S. Geoloical Survey, Washington.
Valdes-Mujica, A., 2008. la bahia y la ciudad. Pasado, presente y futuro de un ecosistema. El pelícano 2 diciembre 2008 4–11.
Van Daele, M., van Welden, A., Moernaut, J., Beck, C., Audemard, F., Sanchez, J., Jouanne, F., Carrillo, E., Malavé, G., Lemus, A., De Batist, M., 2011. Reconstruction of Late-Quaternary sea- and lake-level changes in a tectonically active marginal basin using seismic stratigraphy: The Gulf of Cariaco, NE Venezuela. Mar. Geol. 279 (15), 37–51, 1–4.
Vázquez, F., Sanchez, M., Alexander, H., Delgado, D., 1991. Distribution of Ni, V, and petroleum hydrocarbons in recent sediments from the Veracruz coast, Mexico. Bull. Environ. Contam. Toxicol. 46, 774–781.
Vitousek, P.M., 1994. Beyond global warming: ecology and global change. Ecology 75, 1861–1876.
Wade, B.A., 1976. The Pollution Ecology of the Kingston Harbour, Jamaica. Scientific Report of the U.W.I, vol. 1. O.D.M. Kingston Harbour Research Project, pp. 1972–1975, 2 & 3.
Wang, J., Baskaran, M., Niedermiller, J., 2017. Mobility of 137Cs in freshwater lakes: A mass balance and diffusion study of Lake St. Clair, Southeast Michigan, USA. Geochem. Cosmochim. Acta 218, 323–342.
Webber, M.K., Webber, D.F., 2003. A collection of studies conducted from the Port Royal Marine Laboratory on the status of Kingston Harbour, Jamaica, in relation to continued organic pollution. Bull. Mar. Sci. 73, 2.
Webber, M., Henry, W., Christian, T., 2019. Clean Kingston Harbour: Pipe Dream or Pot of Gold? the Grace Kennedy Foundation Lecture 2019. Grace Kennedy Foundation, p. 134.
Webster, I.T., Hancock, G.J., Murray, A., 1995. Modelling the effect of salinity on radium desorption from sediments. Geochim. Cosmochim. Acta 59 (12), 2469–2476.
Yáñez-Arancibia, A., Zárate Lomeli, D., Gómez Cruz, M., Godínez Orantes, R., Santiago Fandiño, V., 1999. The ecosystem framework for planning and management the Atlantic coast of Guatemala. Ocean Coast Manag. 42, 2–4, 283—317.
Yang, W., Chen, M., Zhang, F., Zhao, X., Fang, Z., Ma, H., 2016. Anthropogenic impacts on sedimentation in Jiaozhou Bay, China. J. Coast Conserv. 20 (6), 501–506.